J|A|C|S ARTICLES

Published on Web 01/29/2009

Dendritic and Linear Macromolecular Architectures for Photovoltaics: A Photoinduced Charge Transfer Investigation

Arpornrat Nantalaksakul,[†] Astrid Mueller,[‡] Akamol Klaikherd,[†] Christopher J. Bardeen,*[,‡] and S. Thayumanavan*[,†]

Departments of Chemistry, University of Massachusetts, Amherst, Massachusetts 01003, and University of California, Riverside, California 92521

Received November 24, 2008; E-mail: thai@chem.umass.edu; christopher.bardeen@ucr.edu

Abstract: Dendrimers have been previously shown to provide significant advantages in both excited-state energy transfer and charge transfer. However, this architecture causes one of the charges to be encapsulated and thus not available for charge separation over long distances. We conceived dendron−rod−coils as scaffolds that could have the architectural advantage of the dendrimers, while still providing a possible conduit for charge separation. In this study, we have designed and synthesized dendron−rod−coil-based donor−chromophore−acceptor triads and have compared these with dendron−rod and rod−coil diads. We have then evaluated the relative abilities of these molecules in photoinduced charge transfer. Our studies reveal that dendron−rod−coil could indeed be the ideal architecture for efficient photoinduced charge separation.

Introduction

Developing strategies for harnessing energy from renewable sources is a significant challenge facing the scientific community, due to the environmental, economic, and national security implications.[1] Photovoltaics is one of the most promising approaches to addressing this issue.[2] Nature provides both the source and the inspiration for a solution in the form of the sun and the photosynthetic apparatus, respectively. Funneling the sequestered energy from the solar radiation to generate an excited state at a reaction center and utilizing this high-energy state to elicit a sequence of charge transfer (CT) events are the key preliminary steps in photosynthesis.[3] The resultant charge-separated state from these events is ultimately used as a source of chemical energy. Thus, the photosynthetic process involves the conversion of solar energy into chemical energy. Although the ultimate goal of photovoltaics is to convert the solar energy to electrical energy, the preliminary steps are essentially the same. Considering the high efficiency of the photoinduced charge transfer events in nature, it is desirable to mimic these efficiencies for photovoltaics. While the biomolecular architectures are very efficient and stable in their native conditions, they are neither robust nor cheap enough to be practical materials for photovoltaics. Therefore, several artificial systems based on covalent,[4] supramolecular,[5] or polymeric[6] arrays of photoactive and electroactive units have been approached.

Relative placement of the photoactive and electroactive functionalities plays an important role in the vectorial photoinduced charge transfer process. While it is conceivable that

[†] University of Massachusetts.
[‡] University of California.

(1) (a) Arunachalam, V. S.; Fleischer, E. L. *MRS Bull.* **2008**, *33*, 261–263. (b) Chang, M. C. Y. *Curr. Opin. Chem. Biol.* **2007**, *11*, 677–684. (c) Walker, T. W. *Chem. Eng. Prog.* **2008**, *104*, S23–S28. (d) Zahedi, A. *Renewable Energy* **2006**, *31*, 711–718. (e) Eisenberg, R.; Nocera, D. G. *Inorg. Chem.* **2005**, *44* (20), special issue on renewable energy. (f) Lewis, N. S.; Nocera, D. G. *Proc. Natl. Acad. Sci. U.S.A.* **2006**, *103*, 15729–15735.

(2) (a) Hepbasli, A. *Renewable Sustainable Energy Rev.* **2008**, *12*, 593–661. (b) Jester, T. L. *Prog. Photovoltaics* **2002**, *10*, 99–106. (c) Senft, D. C. *J. Electron. Mater.* **2005**, *34*, 571–574.

(3) (a) Wasielewski, M. R. *Chem. Rev.* **1992**, *92*, 435–461. (b) Gust, D.; Kramer, D.; Moore, A.; Moore, T. A.; Verrnaas, W. *MRS Bull.* **2008**, *33*, 383–387. (c) Gust, D.; Moore, T. A. *Science* **1989**, *244*, 35–41. (d) Gust, D.; Moore, T. A.; Moore, A. L. *Acc. Chem. Res.* **2001**, *34*, 40–48. (e) Straight, S. D.; Kodis, G.; Terazono, Y.; Hambourger, M.; Moore, T. A.; Moore, A. L.; Gust, D. *Nat. Nanotechnol.* **2008**, *3*, 280–283. (f) Alstrum-Acevedo, J. H.; Brennaman, M. K.; Meyer, T. J. *Inorg. Chem.* **2005**, *44*, 6802–6827. (g) Balzani, V.; Credi, A.; Venturi, M. *ChemSusChem* **2008**, *1*, 26–58. (h) Bard, A. J.; Fox, M. A. *Acc. Chem. Res.* **1995**, *28*, 141–145. (i) Choi, M. S.; Yamazaki, T.; Yamazaki, I.; Aida, T. *Angew. Chem., Int. Ed.* **2004**, *43*, 150–158. (j) Conlan, B.; Wydrzynski, T.; Hillier, W. *Photosynth. Res.* **2007**, *91*, PS213. (k) Lomoth, R.; Magnuson, A.; Sjodin, M.; Huang, P.; Styring, S.; Hammarstrom, L. *Photosynth. Res.* **2006**, *87*, 25–40. (l) van Patten, P. G.; Shreve, A. P.; Lindsey, J. S.; Donohoe, R. J. *J. Phys. Chem. B* **1998**, *102*, 4209–4216.

(4) (a) Hasselman, G. M.; Watson, D. F.; Stromberg, J. R.; Bocian, D. F.; Holten, D.; Lindsey, J. S.; Meyer, G. J *J. Phys. Chem. B* **2006**, *110*, 25430–25440. (b) Kuciauskas, D.; Liddell, P. A.; Lin, S.; Johnson, T. E.; Weghorn, S. J.; Lindsey, J. S.; Moore, A. L.; Moore, T. A.; Gust, D. *J. Am. Chem. Soc.* **1999**, *121*, 8604–8614. (c) Muthukumaran, K.; Loewe, R. S.; Kirmaier, C.; Hindin, E.; Schwartz, J. K.; Sazanovich, I. V.; Diers, J. R.; Bocian, D. F.; Holten, D.; Lindsey, J. S. *J. Phys. Chem. B* **2003**, *107*, 3431–3442. (d) D'Souza, F.; Smith, P. M.; Zandler, M. E.; McCarty, A. L.; Itou, M.; Araki, Y.; Ito, O. *J. Am. Chem. Soc.* **2004**, *126*, 7898–7907. (e) Haycock, R. A.; Yartsev, A.; Michelsen, U.; Sundstrom, V.; Hunter, C. A. *Angew. Chem., Int. Ed.* **2000**, *39*, 3616–3619. (f) Huijser, A.; Suijkerbuijk, B.; Gebbink, R.; Savenije, T. J.; Siebbeles, L. D. A. *J. Am. Chem. Soc.* **2008**, *130*, 2485–2492. (g) Sugou, K.; Sasaki, K.; Kitajima, K.; Iwaki, T.; Kuroda, Y *J. Am. Chem. Soc.* **2002**, *124*, 1182–1183. (h) Ishi-i, T.; Murakami, K.; Imai, Y.; Mataka, S. *Org. Lett.* **2005**, *7*, 3175–3178. (i) Oekermann, T.; Schlettwein, D.; Wohrle, D. *J. Appl. Electrochem.* **1997**, *27*, 1172–1178. (j) Wurthner, F.; Ahmed, S.; Thalacker, C.; Debaerdemaeker, T. *Chem.—Eur. J.* **2002**, *8*, 4742–4750. (k) Baffreau, J.; Leroy-Lhez, S.; Van Anh, N.; Williams, R. M.; Hudhomme, P. *Chem.—Eur. J.* **2008**, *14*, 4974–4992. (l) Elim, H. I.; Jeon, S. H.; Verma, S.; Ji, W.; Tan, L. S.; Urbas, A.; Chiang, L. Y. *J. Phys. Chem. B* **2008**, *112*, 9561–9564. (m) Kuramochi, Y.; Satake, A.; Itou, M.; Ogawa, K.; Araki, Y.; Ito, O.; Kobuke, Y. *Chem.—Eur. J.* **2008**, *14*, 2827–2841.

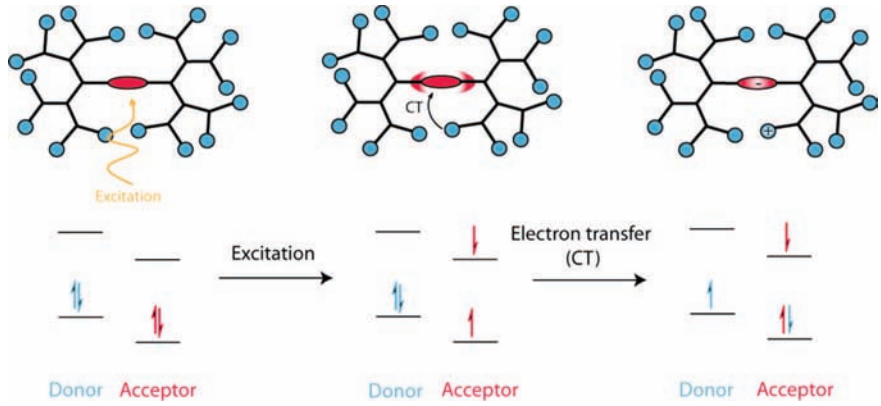

Figure 1. Cartoon showing a charge trap at a core by a dendritic backbone.

one can precisely engineer these in a small molecule, achieving similar control in nonbiological macromolecular systems is very challenging. Dendrimers provide a unique opportunity, since these molecules can be achieved with excellent control in the relative placement of functional groups as well as their molecular weight.[7] In addition, the decreasing density of functional groups from the periphery to the core of the dendrimers is reminiscent of an antenna. Therefore, dendrimers have been extensively investigated as light-harvesting antennae, where excited-state energy from the peripheral functionalities is funneled to the core of a dendrimer.[8] The dendrimers that have been studied for this purpose can be broadly classified into conjugated[9] and nonconjugated[10] dendrimers. Although much more limited, dendrimers have also been investigated as architectures for photoinduced electron transfer processes, the next step in the primary steps of photosynthesis.[11] A schematic of the photoinduced electron transfer process in dendrimers is shown in Figure 1. Although one could envision utilizing a charge-separated species of this type in conversion to chemical energy, such dendritic architectures do not seem ideal for ultimate use in photovoltaics. This is because the charge transfer process causes one of the charges to be localized at the core of the dendrimer (Figure 1). This location in a dendrimer is significantly encapsulated,[12] and therefore, the opportunities for ultimately transporting this charge to an electrode are limited, if any at all. On the other hand, by carrying out a systematic comparison of linear architectures with the corresponding dendrimers, we have also demonstrated that the branched structures indeed provide certain advantages in the photoinduced electron transfer process.[13]

Considering all these features, we asked whether it is possible to envisage a hybrid architecture where we combine the advantages of dendritic structure in the photoinduced electron transfer process with the relatively open nature of the linear polymers for transporting the separated charges. A structure that would fit all these requirements will involve a dendron−rod−coil-based triad, which contains a "rod" chromophore, a "dendron" functionalized with electron-rich moieties, and a polymeric "coil" with electron-poor functionalities (Figure 2). An additional advantage of the dendron−rod−coil architecture is that these structures have been investigated as unique architectures for providing microphase-separated nanoscale architectures,[14] which should provide advantages in our ultimate goal of

(5) (a) Adronov, A.; Frechet, J. M. J. *Chem. Commun.* **2000**, 1701–1710. (b) Aida, T.; Jiang, D. L.; Yashima, E.; Okamoto, Y. *Thin Solid Films* **1998**, *331*, 254–258. (c) Gilat, S. L.; Adronov, A.; Frechet, J. M. J. *Angew. Chem., Int. Ed.* **1999**, *38*, 1422–1427. (d) Hahn, U.; Gorka, M.; Vogtle, F.; Vicinelli, V.; Ceroni, P.; Maestri, M.; Balzani, V. *Angew. Chem., Int. Ed.* **2002**, *41*, 3595–3598. (e) Jiang, D. L.; Aida, T. *Prog. Polym. Sci.* **2005**, *30*, 403–422. (f) Nantalaksakul, A.; Reddy, D. R.; Bardeen, C. J.; Thayumanavan, S. *Photosynth. Res.* **2006**, *87*, 133–150.

(6) (a) Balzani, V.; Ceroni, P.; Maestri, M.; Vicinelli, V. *Curr. Opin. Chem. Biol.* **2003**, *7*, 657–665. (b) Bundgaard, E.; Krebs, F. C. *Sol. Energy Mater. Sol. Cells* **2007**, *91*, 954–985. (c) Colladet, K.; Fourier, S.; Cleij, T. J.; Lutsen, L.; Gelan, J.; Vanderzande, D.; Nguyen, L. H.; Neugebauer, H.; Sariciftci, S.; Aguirre, A.; Janssen, G.; Goovaerts, E. *Macromolecules* **2007**, *40*, 65–72. (d) Gunes, S.; Neugebauer, H.; Sariciftci, N. S. *Chem. Rev.* **2007**, *107*, 1324–1338. (e) Lungenschmied, C.; Dennler, G.; Neugebauer, H.; Sariciftci, S. N.; Glatthaar, M.; Meyer, T.; Meyer, A. *Sol. Energy Mater. Sol. Cells* **2007**, *91*, 379–384. (f) Mayer, A. C.; Scully, S. R.; Hardin, B. E.; Rowell, M. W.; McGehee, M. D. *Mater. Today* **2007**, *10*, 28–33. (g) Peet, J.; Kim, J. Y.; Coates, N. E.; Ma, W. L.; Moses, D.; Heeger, A. J.; Bazan, G. C. *Nat. Mater.* **2007**, *6*, 497–500.

(7) (a) Dykes, G. M. *J. Chem. Technol. Biotechnol.* **2001**, *76*, 903–918. (b) Gittins, P. J.; Twyman, L. *J. Supramol. Chem.* **2003**, *15*, 5–23. (c) Jang, W. D.; Kataoka, K. *J. Drug Delivery Sci. Technol.* **2005**, *15*, 19–30. (d) Klajnert, B.; Bryszewska, M. *Acta Biochim. Pol.* **2001**, *48*, 199–208.

(8) (a) Balzani, V.; Campagna, S.; Denti, G.; Juris, A.; Serroni, S.; Venturi, M. *Acc. Chem. Res.* **1998**, *31*, 26–34. (b) Reference 3i. (c) Dirksen, A.; De Cola, L. *C. R. Chim.* **2003**, *6*, 873–882. (d) Serroni, S.; Campagna, S.; Puntoriero, F.; Loiseau, F.; Ricevuto, V.; Passalacqua, R.; Galletta, M. *C. R. Chim.* **2003**, *6*, 883–893.

(9) (a) Benites, M. D.; Johnson, T. E.; Weghorn, S.; Yu, L. H.; Rao, P. D.; Diers, J. R.; Yang, S. I.; Kirmaier, C.; Bocian, D. F.; Holten, D.; Lindsey, J. S. *J. Mater. Chem.* **2002**, *12*, 65–80. (b) Devadoss, C.; Bharathi, P.; Moore, J. S. *J. Am. Chem. Soc.* **1996**, *118*, 9635–9644. (c) Gronheid, R.; Hofkens, J.; Kohn, F.; Weil, T.; Reuther, E.; Mullen, K.; De Schryver, F. C. *J. Am. Chem. Soc.* **2002**, *124*, 2418–2419. (d) Liu, D. J.; De Feyter, S.; Cotlet, M.; Wiesler, U. M.; Weil, T.; Herrmann, A.; Mullen, K.; De Schryver, F. C. *Macromolecules* **2003**, *36*, 8489–8498. (e) Melinger, J. S.; Pan, Y. C.; Kleiman, V. D.; Peng, Z. H.; Davis, B. L.; McMorrow, D.; Lu, M. *J. Am. Chem. Soc.* **2002**, *124*, 12002–12012. (f) Ranasinghe, M. I.; Varnavski, O. P.; Pawlas, J.; Hauck, S. I.; Louie, J.; Hartwig, J. F.; Goodson, T. *J. Am. Chem. Soc.* **2002**, *124*, 6520–6521. (g) Shortreed, M. R.; Swallen, S. F.; Shi, Z. Y.; Tan, W. H.; Xu, Z. F.; Devadoss, C.; Moore, J. S.; Kopelman, R. *J. Phys. Chem. B* **1997**, *101*, 6318–6322.

(10) (a) Adronov, A.; Gilat, S. L.; Frechet, J. M. J.; Ohta, K.; Neuwahl, F. V. R.; Fleming, G. R. *J. Am. Chem. Soc.* **2000**, *122*, 1175–1185. (b) Choi, M. S.; Aida, T.; Yamazaki, T.; Yamazaki, I. *Chem.—Eur. J.* **2002**, *8*, 2668–2678. (c) Jiang, D. L.; Aida, T. *J. Am. Chem. Soc.* **1998**, *120*, 10895–10901. (d) Neuwahl, F. V. R.; Righini, R.; Adronov, A.; Malenfant, P. R. L.; Frechet, J. M. J. *J. Phys. Chem. B* **2001**, *105*, 1307–1312. (e) Stewart, G. M.; Fox, M. A. *J. Am. Chem. Soc.* **1996**, *118*, 4354–4360.

(11) (a) Capitosti, G. J.; Cramer, S. J.; Rajesh, C. S.; Modarelli, D. A. *Org. Lett.* **2001**, *3*, 1645–1648. (b) Lor, M.; Thielemans, J.; Viaene, L.; Cotlet, M.; Hofkens, J.; Weil, T.; Hampel, C.; Mullen, K.; Verhoeven, J. W.; Van der Auweraer, M.; De Schryver, F. C. *J. Am. Chem. Soc.* **2002**, *124*, 9918–9925. (c) Sadamoto, R.; Tomioka, N.; Aida, T. *J. Am. Chem. Soc.* **1996**, *118*, 3978–3979. (d) Guldi, D. M.; Swartz, A.; Luo, C.; Gómez, R.; Segura, J.; Martín, N. *J. Am. Chem. Soc.* **2002**, *124*, 10875. (e) Qu, J.; Pschirer, N. G.; Liu, D.; Stefan, A.; De Schryver, F. C.; Müllen, K. *Chem.—Eur. J.* **2004**, *10*, 528.

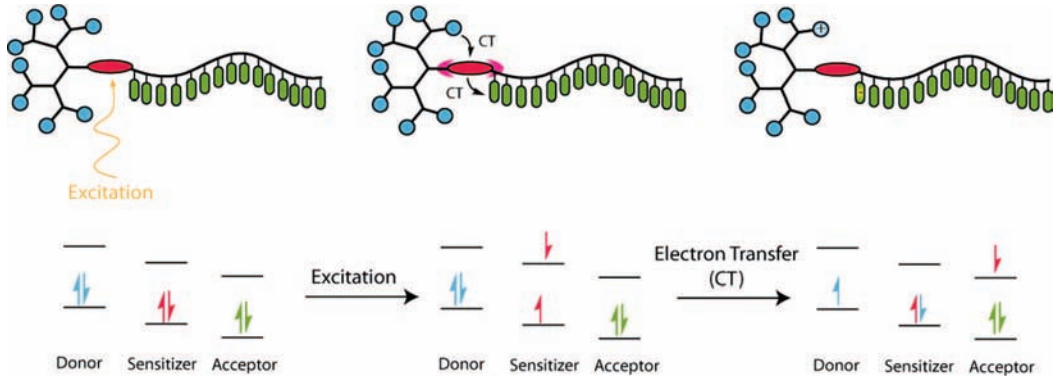

Figure 2. Cartoon showing an electron transfer process in dendron−rod−coils.

photovoltaic devices. In this paper, we describe our molecular design, syntheses, and evaluation of the relative roles of the dendritic and the linear polymer component in the photoinduced electron transfer processes. Our results show that the dendron−rod−coil combination does indeed provide unique advantages in photoinduced charge transfer.

For photoinduced charge transfer in the dendron−rod−coil molecule, it is necessary that the electron-rich functionality in the dendron is capable of reducing the excited state of the rod chromophore and the electron-poor functionality of the coil is capable of oxidizing this excited state as shown in Figure 2. From a frontier molecular orbital perspective, this means that the highest occupied molecular orbital (HOMO) of the electron-donating dendron functionality should be higher than that of the chromophore and the lowest unoccupied molecular orbital (LUMO) of the electron-accepting polymer coil functionality should be lower than that of the rod chromophore. Accordingly, (diarylamino)pyrene was chosen as the electron-rich functionality (electron donor) on the dendritic periphery, naphthalenediimide as the electron-poor functionality (electron acceptor) in the polymer coil, and benzthiadiazole as the rod chromophore (sensitizer). Thus, our target structures are shown as **1**−**3** in Chart 1.

Results and Discussion

Synthesis and Characterization. When assembling a macromolecule with different components, such as the ones shown in Chart 1, it is advantageous to approach the synthesis in a modular fashion. The modular approach allows for flexibility in varying the functional groups in molecules with relative ease, which then facilitates structure−property relationship studies. Thus, the (diarylamino)pyrene-based dendron, the benzthiadiazole-based rod, and the naphthalenediimide-bearing polymer coil were synthesized separately and then assembled in the final steps of the synthesis to obtain the desired dendron−rod−coils. The key step in our modular approach is to be able to differentially substitute the polymer coil and the dendron onto a symmetrical core chromophore. It is necessary that we use a set of complementary and versatile reactions to carry out these substitutions. We envisaged the possibility of using a simple alkylation reaction to substitute the dendron onto the chromophore, while utilizing the 1,3-dipolar cycloaddition reaction between an azide and an alkyne (the so-called "click chemistry") to install the polymer coil.

Considering our targets, it is necessary that the rod chromophore be desymmetrized, presenting a phenolic moiety at one terminus, while presenting an alkynyl functionality at the other. To achieve this, we simply synthesized the symmetrical dihydroxy-functionalized benzthiadiazole chromophore **6** using our previously reported procedure.[15] Chromophore **6** was then reacted with a deficient amount of propargyl bromide in the presence of K_2CO_3 and 18-crown-6. This reaction afforded the targeted unsymmetrical chromophore **7**, as shown in Scheme 1. The remaining phenolic functionality on the rod chromophore will be subjected to the alkylation reaction with bromomethyl-functionalized dendrons, while the propargyl group will be utilized to attach the polymer coil via 1,3-dipolar cycloaddition or click reaction with azide-terminated polymers to obtain the desired dendron−rod−coils as final products.

The polymer coil contains a naphthalenediimide (NDI) as the side chain functionality on a polymethacrylate backbone. To attach this polymer to the chromophore through the cycloaddition reaction, it is necessary that one of the chain ends contains

(12) (a) Cameron, C. S.; Gorman, C. B. *Adv. Funct. Mater.* **2002**, *12*, 17–20. (b) Cardona, C. M.; Mendoza, S.; Kaifer, A. E. *Chem. Soc. Rev.* **2000**, *29*, 37–42. (c) Valerio, C.; Fillaut, J. L.; Ruiz, J.; Guittard, J.; Blais, J. C.; Astruc, D. *J. Am. Chem. Soc.* **1997**, *119*, 2588–2589. (d) Chasse, T. L.; Sachdeva, R.; Li, C.; Li, Z. M.; Petrie, R. J.; Gorman, C. B. *J. Am. Chem. Soc.* **2003**, *125*, 8250–8254. (e) Diederich, F.; Felber, B. *Proc. Natl. Acad. Sci. U.S.A.* **2002**, *99*, 4778–4781. (f) Gorman, C. B. *C. R. Chim.* **2003**, *6*, 911–918. (g) Hecht, S.; Frechet, J. M. J. *Angew. Chem., Int. Ed.* **2001**, *40*, 74–91. (h) Hong, Y. R.; Gorman, C. B. *Langmuir* **2006**, *22*, 10506–10509. (i) Kaifer, A. E. *Eur. J. Inorg. Chem.* **2007**, 5015–5027. (j) Ong, W.; Kaifer, A. E. *Angew. Chem., Int. Ed.* **2003**, *42*, 2164–2167. (k) Schenning, A.; Arndt, J. D.; Ito, M.; Stoddart, A.; Schreiber, M.; Siemsen, P.; Martin, R. E.; Boudon, C.; Gisselbrecht, J. P.; Gross, M.; Gramlich, V.; Diederich, F. *Helv. Chim. Acta* **2001**, *84*, 296–334. (l) Bryce, M. R.; Devonport, W.; Goldenberg, L. M.; Wang, C. S. *Chem. Commun.* **1998**, 945–951. (m) Daniel, M. C.; Ruiz, J.; Astruc, D. *J. Am. Chem. Soc.* **2003**, *125*, 1150–1151. (n) Gonzalez, B.; Cuadrado, I.; Casado, C. M.; Alonso, B.; Pastor, C. J. *Organometallics* **2000**, *19*, 5518–5521. (o) Hogan, C. F.; Harris, A. R.; Bond, A. M.; Sly, J.; Crossley, M. J. *Phys. Chem. Chem. Phys.* **2006**, *8*, 2058–2065. (p) Nijhuis, C. A.; Yu, F.; Knoll, W.; Huskens, J.; Reinhoudt, D. N. *Langmuir* **2005**, *21*, 7866–7876.

(13) (a) Ahn, T. S.; Nantalaksakul, A.; Dasari, R. R.; Al-Kaysi, R. O.; Muller, A. M.; Thayumanavan, S.; Bardeen, C. J. *J. Phys. Chem. B* **2006**, *110*, 24331–24339. (b) Nantalaksakul, A.; Dasari, R. R.; Ahn, T. S.; Al-Kaysi, R.; Bardeen, C. J.; Thayumanavan, S. *Org. Lett.* **2006**, *8*, 2981–2984.

(14) (a) Cho, B. K.; Jain, A.; Gruner, S. M.; Wiesner, U. *Science* **2004**, *305*, 1598–1601. (b) Lecommandoux, S.; Klok, H. A.; Sayar, M.; Stupp, S. I. *J. Polym. Sci., Part A: Polym. Chem.* **2003**, *41*, 3501–3518. (c) Messmore, B. W.; Hulvat, J. F.; Sone, E. D.; Stupp, S. I. *J. Am. Chem. Soc.* **2004**, *126*, 14452–14458. (d) Tian, L.; Hammond, P. T. *Chem. Mater.* **2006**, *18*, 3976–3984. (e) Tian, L.; Nguyen, P.; Hammond, P. T. *Chem. Commun.* **2006**, 3489–3491. (f) Zubarev, E. R.; Sone, E. D.; Stupp, S. I. *Chem.—Eur. J.* **2006**, *12*, 7313–7327. (g) Zubarev, E. R.; Stupp, S. I. *J. Am. Chem. Soc.* **2002**, *124*, 5762–5773.

(15) Thomas, K. R. J.; Thompson, A. L.; Sivakumar, A. V.; Bardeen, C. J.; Thayumanavan, S. *J. Am. Chem. Soc.* **2005**, *127*, 373–383.

Chart 1. Structures of Dendron−Rod−Coils Used in These Studies

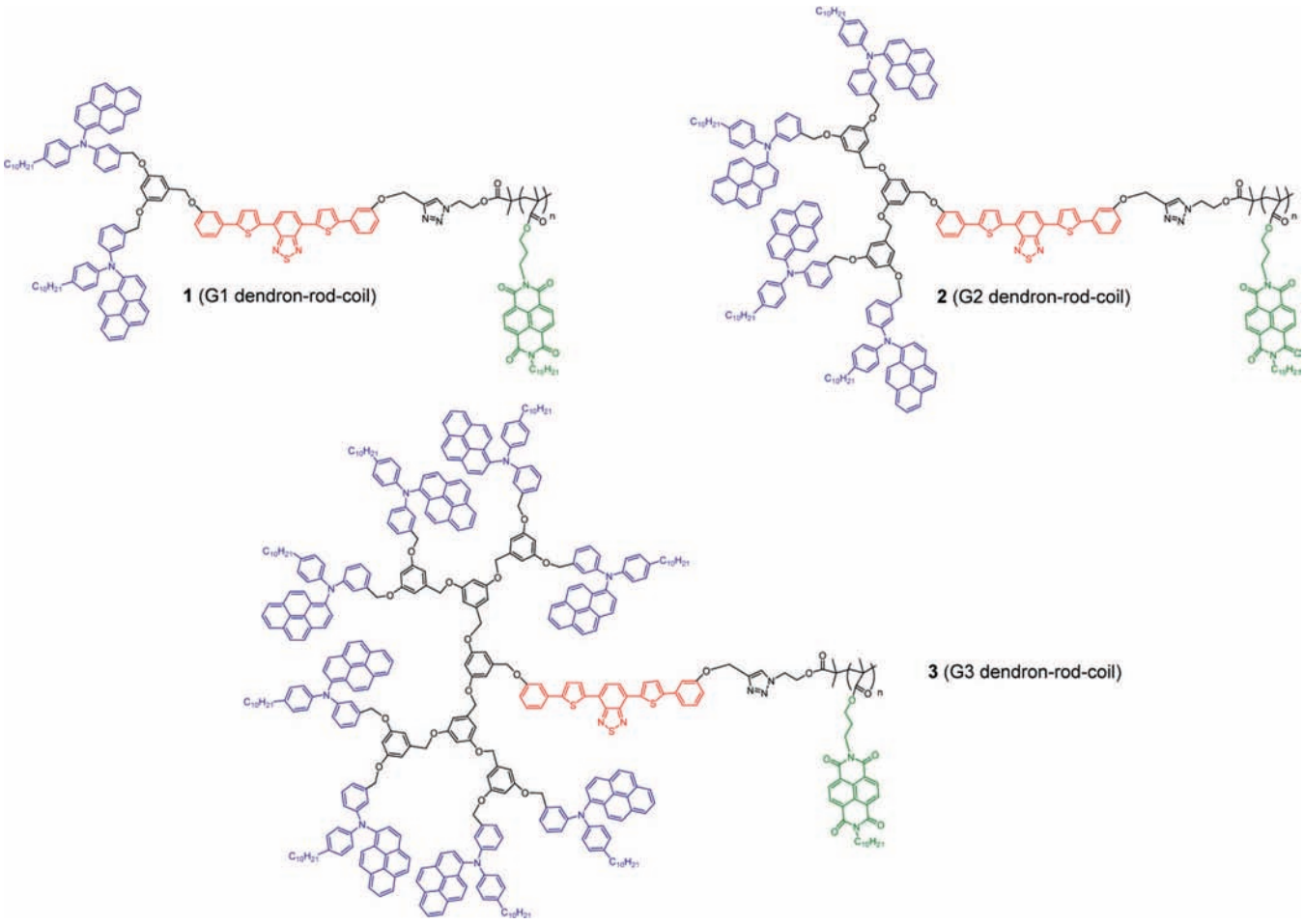

Scheme 1. Unsymmetrical Substitution of Rod Species

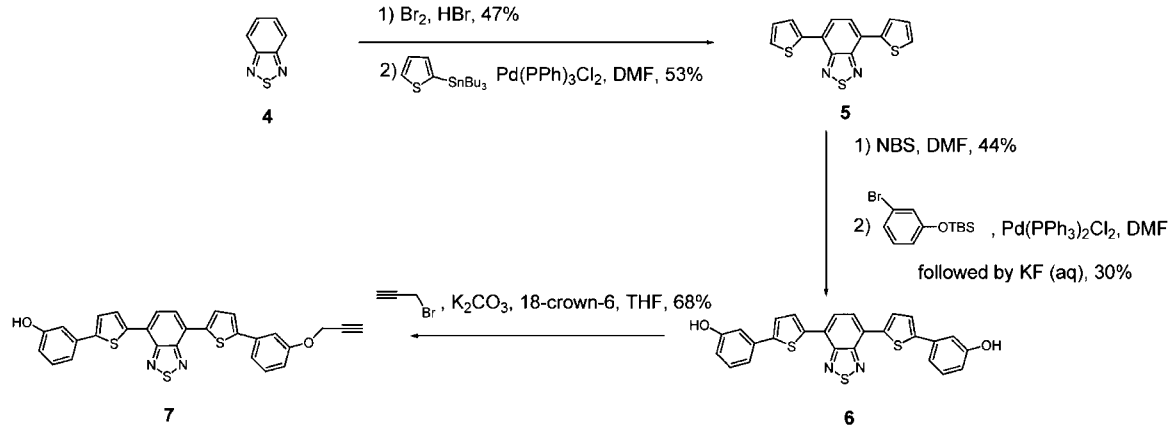

an azide functionality. We utilized atom transfer radical polymerization (ATRP),[16] a living radical polymerization technique, that not only allows for selective incorporation of a single functionality at the initiator end of the polymer, but also can be used for the synthesis of methacrylate polymers with very good control over their polydispersities. Thus, we used 2-azidoethyl bromoisobutyrate (**11**) as the initiator for the synthesis of the methacrylate-based naphthalenediimide polymer. To incorporate naphthalenediimide as the side chain to the methacrylate monomer, we first targeted the molecule **9** that contains a single hydroxyalkyl functionality. This group will serve as the handle to install the naphthalenediimide functionality onto a polymerizable unit by treatment with methacryloyl chloride to obtain compound **10** (Scheme 2). Polymerization of **10** using **11** as the initiator in the presence of cuprous bromide and PMDETA afforded the polymer **12** in 61% yield with a PDI of 1.14 and M_n of 9326.

While the polymer will be incorporated onto the chromophore core through the cycloaddition reaction, the dendron will be incorporated onto the chromophore using the Williamson ether

(16) (a) Coessens, V.; Pintauer, T.; Matyjaszewski, K. *Prog. Polym. Sci.* **2001**, *26*, 337–377. (b) Pintauer, T.; Matyjaszewski, K. *Chem. Soc. Rev.* **2008**, *37*, 1087–1097.

Scheme 2. Synthesis of Polymer Containing Pendant NDI Units

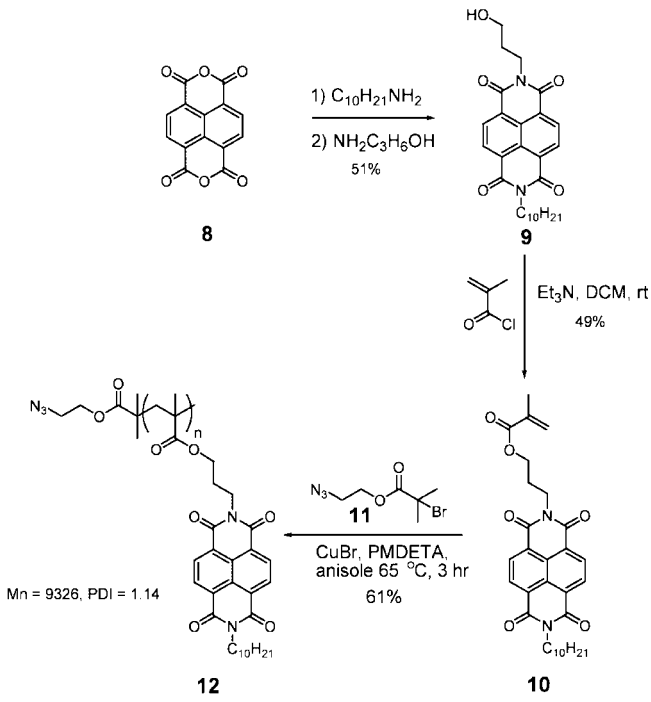

synthesis. Since the chromophore core will be synthesized with a phenolic functionality, the targeted dendrons should have a bromoalkyl moiety at their focal point. We have previously reported the syntheses of dendrons **13**−**15** containing (diarylamino)pyrene units in the periphery and a bromomethyl functionality at the focal point.[15] These dendrons were treated with the monophenolic chromophore core **7** under the Williamson alkylation conditions to obtain the dendron−rod components, which were further reacted with azide-terminated polymers under click chemistry conditions to obtain the dendron−rod−coils **1**−**3** (Scheme 3). Note that if the polymeric coils were first installed onto the rod moiety to obtain rod−coil precursors, the overall synthetic steps would be reduced since the difference in **1**−**3** arises from the dendron. However, the separation of the rod−coils from the desired dendron−rod−coils in the final step is likely to be problematic from our experience with these molecules. Alternatively, separation of these dendron−rods from the final dendron−rod−coils was possible with a conventional chromatographic method due to the significant difference in polarity between these two species.

All newly synthesized compounds were characterized by ^{1}H and ^{13}C NMR. Additionally, the purity of all targeted compounds was elucidated using gel permeation chromatrography (GPC) (Figure 3). All dendron−rod−coil species showed a single peak which was shifted toward the higher molar mass region compared to those of their polymeric parent species, as shown in Figure 3. The molar mass of dendron−rod−coils was also found to be equivalent to the sum of the molar masses of their corresponding dendron−rod species and polymeric coil with similar PDIs. This evidence implied that dendron−rod−coils were successfully synthesized. The molar masses (M_n) of all dendron−rod−coils along with dendron−rod and polymeric-coil species are shown in Table 1.

Dendron−rod−coils were also characterized using linear absorption spectroscopy. The naphthalenediimide functionality exhibits an absorption maximum around 381 nm, (diarylamino)pyrene at 380 nm, and the benzthiadiazole chromophore at 490 nm (Figure 4). If one physically mixes the three components, i.e., the dendron, the chromophore rod, and the polymer coil, the spectrum obtained from these mixtures matches very well with that of the dendron−rod−coil molecule. This not only provides additional support for characterizing the structure, but also suggests that there is no electronic communication among the (diarylamino)pyrene, benzthiadiazole, and naphthalenediimide functionalities in the ground state. This is understandable, because the linkages between these photo- and electroactive functionalities are nonconjugated.

Relative Energy Levels of the Functionalities for Photoinduced Electron Transfer. For photoinduced charge transfer to occur from the excited state of the chromophore rod, the positioning of the frontier orbital energy levels of the (diarylamino)pyrene and the naphthalenediimide units relative to the benzthiadiazole chromophore core is appropriate, as shown in Figure 2. The positioning of the HOMO or the LUMO of a functionality can be estimated electrochemically by measuring its oxidation or reduction potential, respectively. Once one of the frontier orbital energy levels is determined, the energy level of the other orbital can be determined by estimating the HOMO−LUMO gap. This gap can be taken to be equivalent to ΔE_{0-0}, which is arrived at using the absorption and emission spectra of the photoactive or electroactive molecules. To estimate the energy levels of (diarylamino)pyrene **16**, naphthalenediimide **9** and the benzthiadiazole chromophore **17** molecules were used as the control structures (Figure 5a). Cyclic voltammograms of these molecules are shown in Figure 5b. The onset oxidation potential of molecules **16** and **17** were 535 and 860 mV, respectively, and the onset reduction potential of molecule **9** was −665 mV. The intersection of the absorption and emission spectra of these molecules are taken to be the ΔE_{0-0} gap, the values of which are listed in Table 2. These values, in combination with the redox potential from cyclic voltammetry, were used to estimate the energy of both the HOMO and LUMO levels of functionalities **9**, **16**, and **17**. Using the value of 4.41 V as the offset value, the HOMO and the LUMO energy levels relative to a vacuum are listed in Table 2. These energy levels, graphically shown in Figure 5c, clearly indicate that the excited state of the chromophore **17** can be reduced by the (diarylamino)pyrene **16** or oxidized by the naphthalenediimide **9**. Therefore, it is thermodynamically feasible that the excitation of the benzthiadiazole chromophore results in a photoinduced charge-separated state, where the positive charge is at the (diarylamino)pyrene functionality in the dendron and the negative charge is at the naphthalenediimide functionality. In the following sections, we equate our excited-state quenching to arise from a photoinduced charge transfer event. The two limiting mechanisms that are commonly implicated in excited-state quenching are (i) electronic energy transfer from a high-energy chromophore to a lower energy one and (ii) charge transfer from or to the excited state of the chromophore. The relative energy levels of the chromophore and the charge transfer units, estimated in Figure 5 and Table 2, show that an energy transfer process is not thermodynamically feasible from the chromophore core to the (diarylamino)pyrene or the naphthalenediimide functionalities, as the latter molecules exhibit higher band gaps. Therefore, it is reasonable that the observed excited-state quenching is indeed due to a charge transfer process. The Stern−Volmer quenching experiments of **17** using **9** or **16** as quenchers provide additional support for this (vide infra).

Scheme 3. Synthesis of Dendron−Rod−Coil Species

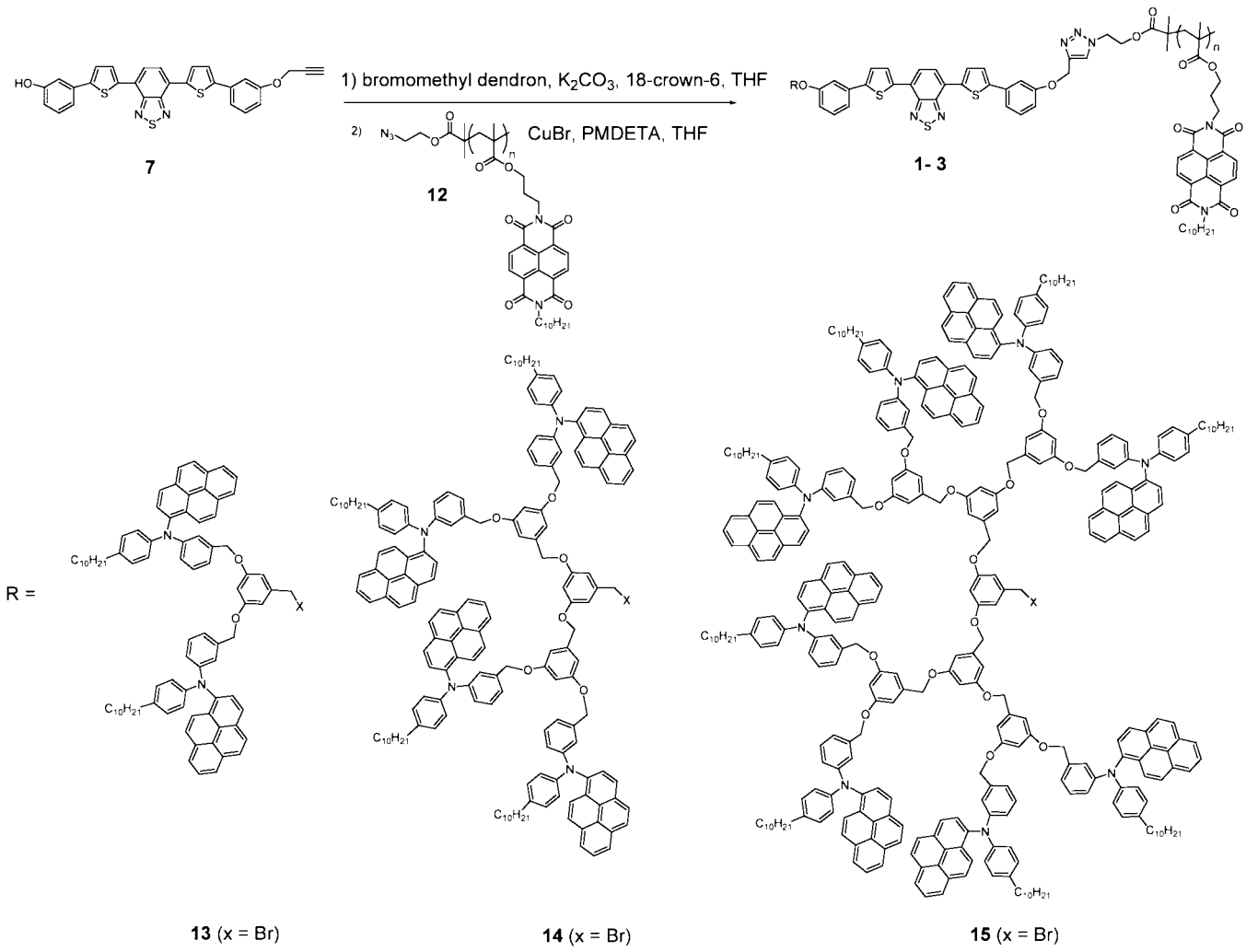

Steady-State and Time-Resolved Spectroscopy. To investigate whether the photoinduced electron transfer process is observed in these molecules, we analyzed the emission spectra of molecules **1**−**3** relative to that of the control chromophore **17**. At similar absorbance with respect to the benzthiadiazole chromophore absorption at 490 nm, the emission centered at 603 nm from the molecules **1**−**3** was considerably more quenched relative to that of **17**, as exemplified in Figure 6a. This observation provided the preliminary qualitative indication that incorporating an electron-rich dendron and the electron-poor polymeric coil is indeed effective for photoinduced charge separation. The extent of photoinduced electron transfer based quenching was quantified using time-resolved studies (vide infra).

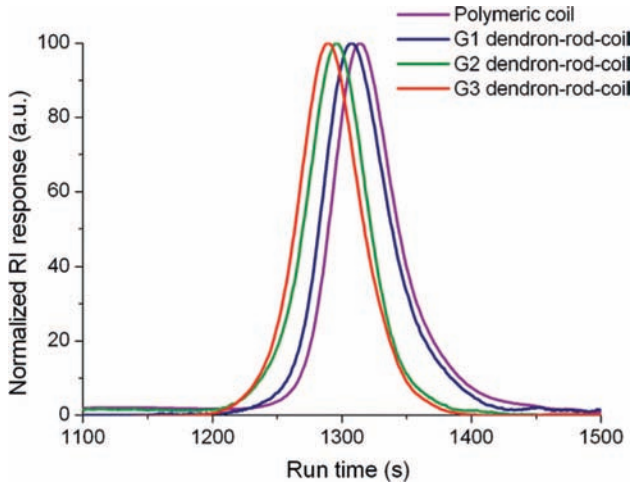

Figure 3. GPC profiles of G1−G3 dendron−rod−coils compared to their parent polymeric species in THF.

Next, we were interested in identifying whether it is the dendron or the coil that contributes the most to the observed photoinduced charge transfer based quenching. To analyze this, we synthesized dendron−rod and rod−coil counterparts to the dendron−rod−coil molecules **1**−**3**. Structures of these molecules are shown in Figure 6c. The emission spectra of the

Table 1. Molar Masses (M_n) and PDIs of All Compounds Obtained by GPC (THF)

molecule	M_n[a]	PDI
polymeric coil **12**	9326	1.14
G1 dendron−rod **18**	1777	1.03
G2 dendron−rod **19**	3321	1.03
G3 dendron−rod **20**	5193	1.02
G1 dendron−rod−coil **1**	10825	1.07
G2 dendron−rod−coil **2**	12940	1.05
G3 dendron−rod−coil **3**	13186	1.09

[a] M_n is estimated using PMMA standards.

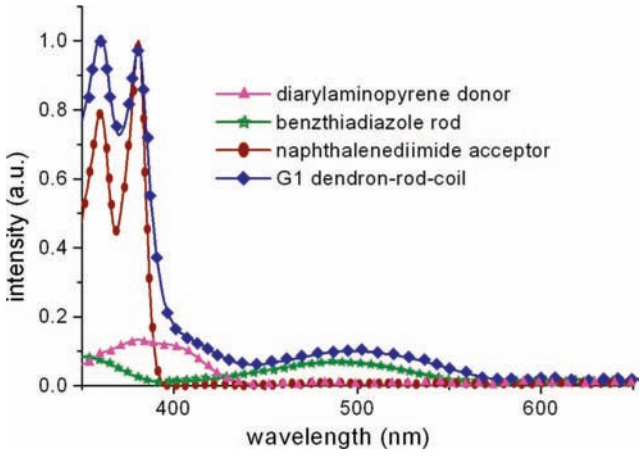

Figure 4. Absorption spectra of the G1 dendron−rod−coil and its chromophore constituents.

chromophore **17**, G1 dendron−rod−coil **1**, G1 dendron−rod **18**, and rod−coil molecule **21** are compared in Figure 6b. These results qualitatively indicate that the combination of the dendron and the polymeric coil is much better in the emission quenching. To quantify the efficiency of photoinduced charge transfer and evaluate the relative contributions from the dendron and the coil, we have carried out time-resolved fluorescence measurements.

As with the steady-state measurements shown above, time-resolved fluorescence measurements were also carried out in dichloromethane. As mentioned earlier, the fluorescence decays observed here are due to the charge transfer from (diarylamino)pyrene (DAP) and naphthalenediimide (NDI) to the excited state of the benzthiadiazole rod. All observed fluorescence decays are nonexponential, which implies the distribution of conformations of both the benzyl ether dendron and methacrylate

Table 2. Band Gaps and Frontier Energy Levels of **16**, **17**, and **19**

functionality	ΔE_{0-0} (eV)	*E*(HOMO) (eV)	*E*(LUMO) (eV)
(diarylamino)pyrene **16**	2.8	−5.0	−2.2
benzthiadiazole chromophore **17**	2.3	−5.3	−3.0
naphthalenediimide **9**	3.2	−7.0	−3.8

polymeric backbone owing to their flexibility. This behavior is consistent with previous observations from our group and others.[15,17] To fit these nonexponential decays, biexponential functions of the form $Ae^{-1/\tau_A} + B^{-1/\tau_B}$ were used; the results of our fits are given in Table 3. As we have done previously,[13,15] we parametrize our biexponential decay dynamics using a single "average" decay rate, k_{acc}, defined as

$$k_{acc} = \frac{A+B}{A\tau_A + B\tau_B} \quad (1)$$

Once we have the average decay rate, k_{acc}, we can also define an effective quenching rate, k_Q:

$$k_Q = k_{acc} - k^0_{acc} \quad (2)$$

where k^0_{acc} is the fluorescence decay of the bare benzthiadiazole rod in the absence of both donor and acceptor quenchers. The efficiencies of charge transfer in dendron−rod−coils in all generations were calculated using the relationship

$$\eta_{CT} = \frac{k_Q}{k_{acc}} \quad (3)$$

From the data in Table 3, several noteworthy trends can be discerned. First, the overall fluorescence quenching rate k_Q is larger in the dendron−rod−coil molecules than in the dendron−rod molecules in all cases. The hypothesis put forward in the Introduction, that the addition of the NDI coil would enhance

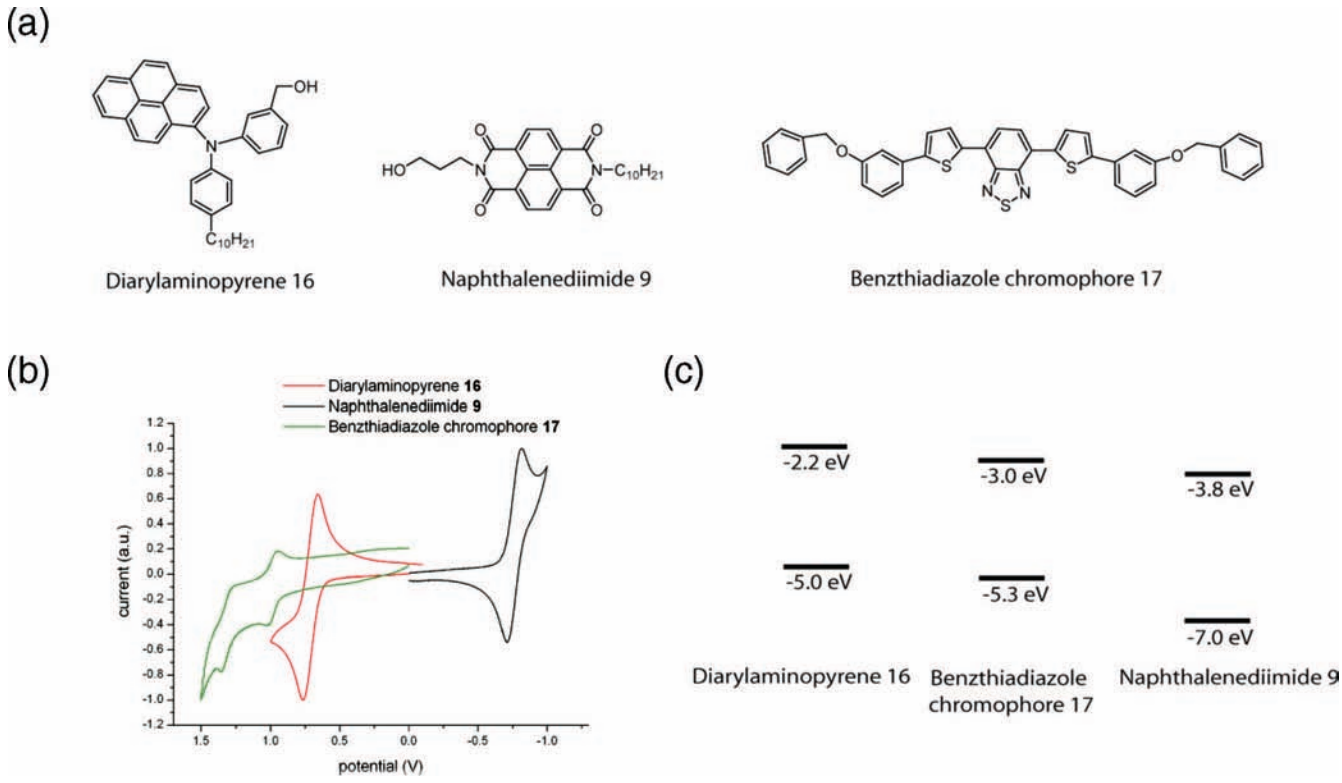

Figure 5. (a) Structures of the model molecules investigated, (b) cyclic voltammogram in dichloromethane with respect to Ag/Ag^+, and (c) relative energy levels of the molecules **9**, **16**, and **17**.

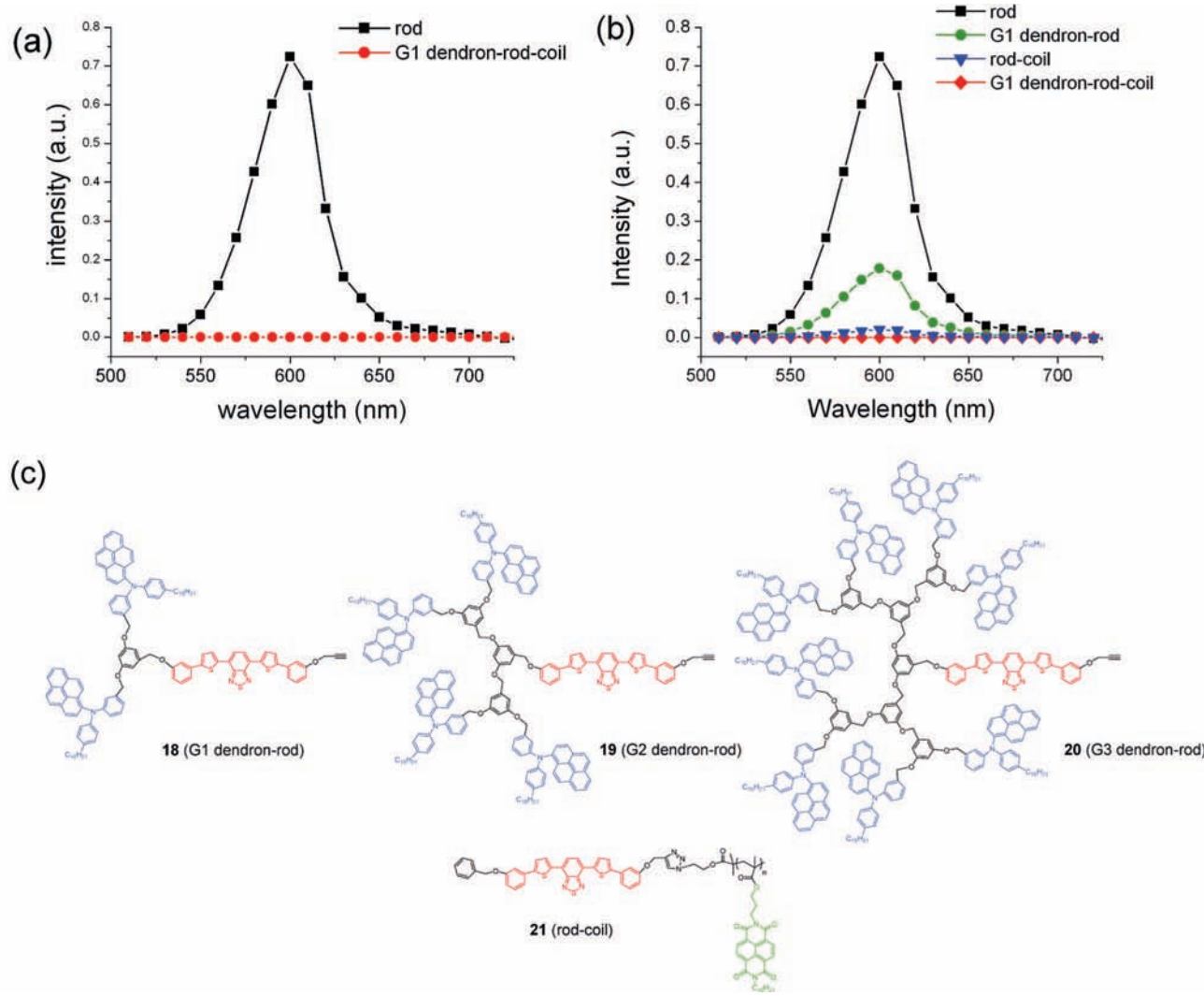

Figure 6. (a) Emission spectra of the G1 dendron−rod−coil compared to that of the rod. (b) Emission spectra of the G1 dendron−rod−coil, G1 dendron−rod, and rod−coil compared to that of the rod. All steady-state measurements were carried out in dichloromethane (excitation wavelength 500 nm). (c) Structures of the G1−G3 dendron−rods and the rod−coil.

Table 3. Rod Fluorescence Decay (Excited at 500 nm) and CT Efficiencies

entry	molecule	A	τ_A (ns)	B	τ_B (ns)	k_Q (ns^{-1})	η_{CT}
1	rod **17**		7.66				
2	G1 dendron−rod **18**	0.32	1.24	0.68	3.56	0.23	0.65
3	G2 dendron−rod **19**	0.41	0.82	0.59	2.88	0.36	0.74
4	G3 dendron−rod **20**	0.56	0.73	0.44	3.24	0.42	0.77
5	G1 dendron−rod−coil **1**	0.56	0.74	0.44	2.90	0.47	0.79
6	G2 dendron−rod−coil **2**	0.60	0.64	0.40	2.65	0.57	0.82
7	G3 dendron−rod−coil **3**	0.59	0.62	0.41	2.92	0.51	0.80
8	rod−coil **21**	0.49	0.74	0.51	3.95	0.29	0.70
9	G1 dendrimer **22**	0.64	5.36	0.36	1.95	0.12	0.48
10	G2 dendrimer **23**	0.62	4.76	0.38	0.98	0.18	0.58
11	G3 dendrimer **24**	0.60	5.49	0.40	1.00	0.15	0.54

charge transfer, is apparently correct. The total quenching rate, however, is not the sum of the individual contributions from the NDI and DAP moieties. This can be seen from the data in Table 3 for the G1 compounds. The sum of the k_Q values for the dendron−rod and rod−coil molecules, 0.23 ns^{-1} + 0.29 ns^{-1} = 0.52 ns^{-1}, is greater than 0.47 ns^{-1}, which is the experimental value for the G1 dendron−rod−coil. This discrepancy becomes even more pronounced for later generations, and in the G3 molecules the expected k_Q is 0.71 ns^{-1}, as compared to 0.51 ns^{-1} as measured experimentally. The beneficial effect of larger dendrons on charge transfer appears to be suppressed in the dendron−rod−coil molecules. This can also be seen from the trends in η_{CT} in Table 3. Moreover, when comparing the abilities of the dendritic donor and the acceptor to quench the excited state of the chromophore in dendron−rods and rod−coils, respectively, it is clear that dendrons are more efficient in photoinduced electron transfer than the acceptor polymer, except in the case of G1 dendron−rod−coil **1**. Therefore, it is intuitively appropriate to assume that the dendron−chromophore−dendron triad (structures in Figure 7) should be more efficient than dendron−rod−coil molecules, at least with higher generation dendrimers.

We have previously studied the dendron−chromophore−dendron triad.[15] Surprisingly, the charge transfer efficiencies of the dendritic triads **22**−**24** are much worse than the corresponding dendron−rod−coil triads **1**−**3**. One could rationalize this observation on the basis of the fact that the dendron−rod−coil

(17) (a) Lee, K. C. B.; Siegel, J.; Webb, S. E. D.; Leveque-Fort, S.; Cole, M. J.; Jones, R.; Dowling, K.; Lever, M. J.; French, P. M. W. *Biophys. J.* **2001**, *81*, 1265–1274. (b) Phillips, J. C. *Rep. Prog. Phys.* **1996**, *59*, 1133–1207. (c) Lakowicz, J. R. *Principles of Fluorescence Spectroscopy*, 2nd ed.; Kluwer: New York, 1999.

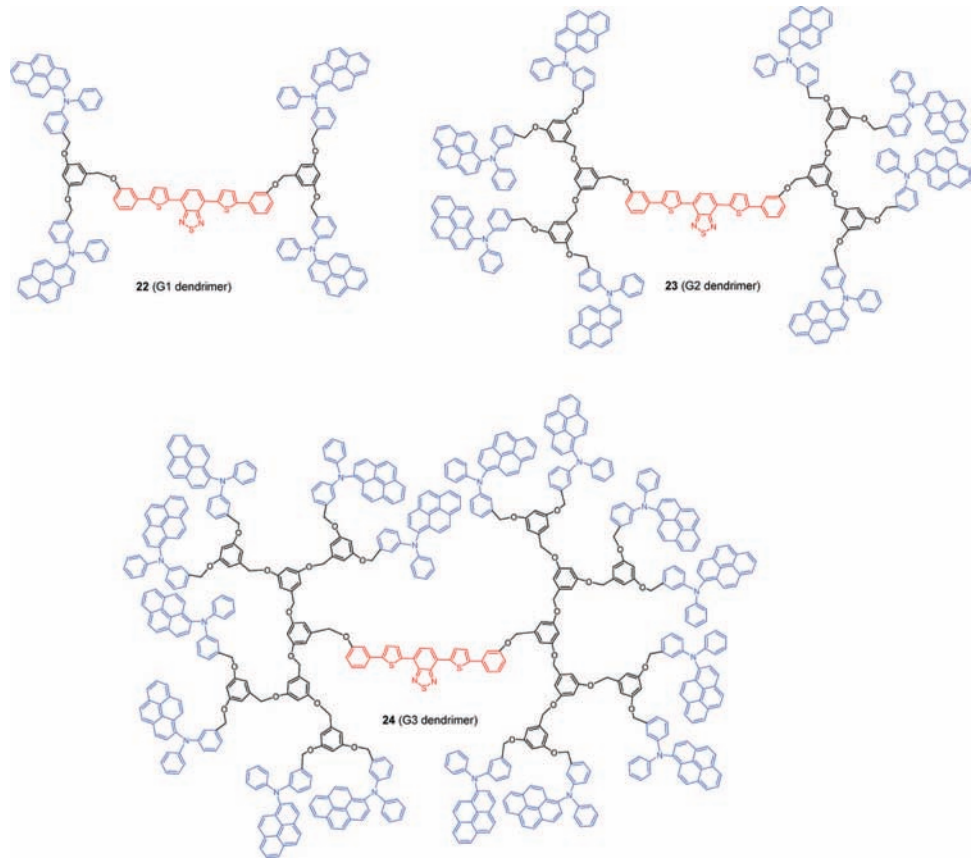

Figure 7. Structures of the donor−chromophore−donor dendrimer triad.

is a donor−chromophore−acceptor triad, whereas the dendritic triad is a donor−chromophore−donor triad. However, it is even more interesting that the η_{CT} for the dendritic triads **22**−**24** are less than those of the dendron−rod-based donor−chromophore diad molecules **18**−**20**. The question then is why installing large dendron-containing DAP groups on one side of the chromophore in dendron−rod−coils does not result in as large an enhancement of electron transfer efficiency as one would expect and installing two of them on the chromophore in dendritic triads leads to even a decrease in the electron transfer efficiency.

One could rationalize the observed results using back-folding and steric interference. We know there exist multiple conformations in both the DAP dendrons and the NDI coil on the basis of their nonexponential fluorescence decays. We have previously shown that, as the size of the dendron increases, two competing factors contribute to the overall CT quenching rate. First, the local density of the quenchers increases (raising k_Q), but also their average distance increases (lowering k_Q). If we now add a third factor, the presence of a large group on the opposite side of the benzthiadiazole core (either the NDI coil or the DAP dendron), it is reasonable to expect that this large, flexible group would interfere with DAP's ability to access the core and thus further suppress the expected increase in k_Q with generation. Thus, we believe that conformational congestion in both the dendron−rod−coil and the dendron−rod−dendron molecules prevents the favorable scaling of k_Q with generation observed in the dendron−rod molecules. Figure 8 compares k_Q in different species. The greater difference between k_Q(dendron−rods) + k_Q(rod−coils) and k_Q(dendron−rod−coils) (Figure 8a) as well as between k_Q(dendron−rod) and k_Q(dendrimers) (Figure 8b) in high-generation dendrons where steric congestion plays a more significant role in the rate of electron transfer provides support for this hypothesis.

In any case, it is clear from Table 3 that the dendron−rod−coils are architecturally better at quenching the excited state of the chromophore rod (Figure 9). We were interested in identifying the relative contribution by each of the structural components, i.e., the dendron and the polymer coil, to the overall photoinduced charge transfer based fluorescence quenching process. We utilized the relative charge transfer rates for the dendron−rod diads **18**−**20** and the rod−coil diad **21** to estimate the possible relative contribution. The assumption here is that these diad rates are useful estimates of the effective contribution of the electron donor and the acceptor to the photoinduced charge transfer process in the triads **1**−**3**. As we have mentioned above, the contributions by the dendrons are indeed affected by the presence of the coil, and we therefore note that this assumption is not foolproof. However, we estimated the relative contributions to gain some insight into the architectural contributions by the dendrons and the coils in the photoinduced charge transfer processes. The estimates are shown in Table 4.

From Table 4, one can conclude that the contributions from the dendron and the polymer coil are about the same. However, it should be noted that there is another variation in the triad molecules in addition to the architectural variation (dendron vs polymer). It involves the relative ability of the (diarylamino)pyrene as the electron donor to quench the excited state of the benzthiadiazole chromophore, compared to that of the naphthalenediimide functionality as the electron acceptor. We carried out Stern−Volmer quenching experiments to identify the relative abilities of these functionalities to quench the excited state of benzthiadiazole through charge transfer. In this experiment, the

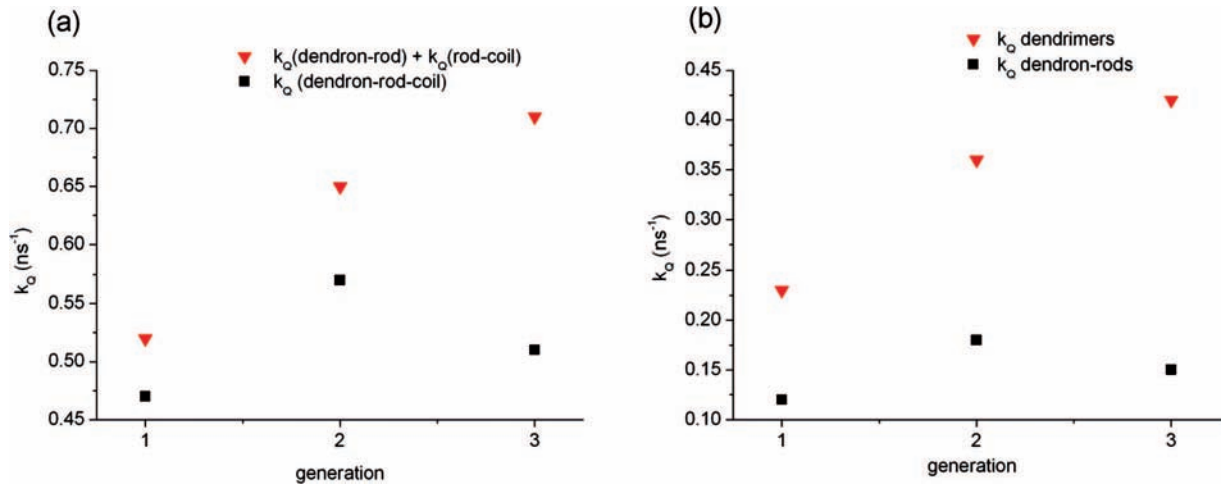

Figure 8. Comparison between (a) k_Q(dendron−rods) + k_Q(rod−coils) and k_Q(dendron−rod−coils) and (b) k_Q(dendrimers) and k_Q(dendron−rods).

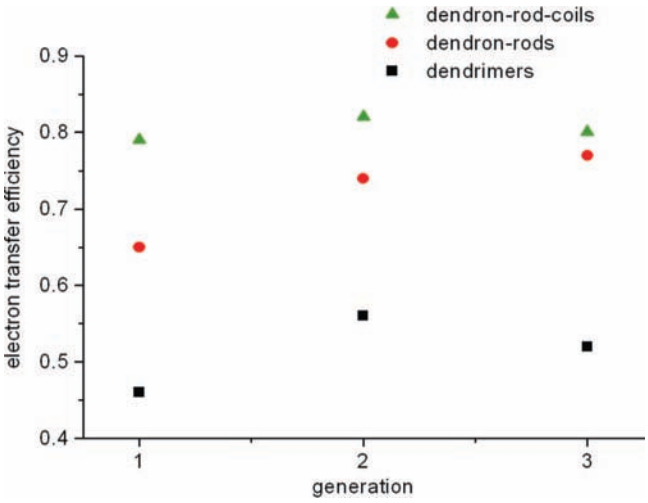

Figure 9. Electron transfer efficiency in different species and different generations.

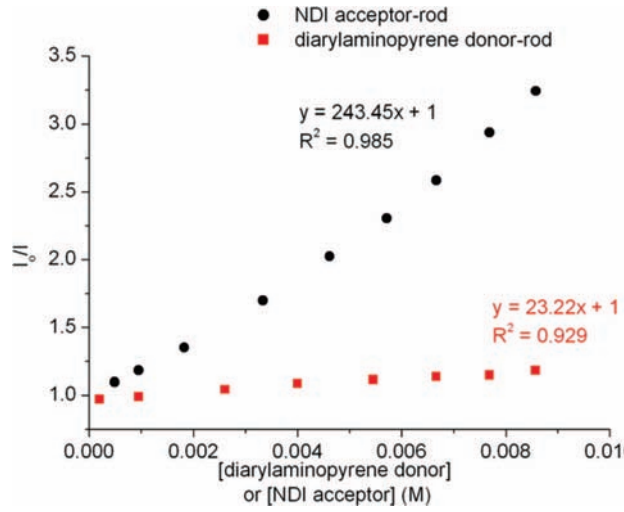

Figure 10. Stern−Volmer plots of the NDI acceptor−rod and DAP donor−rod with the chromophore.

Table 4. Comparison of CT Kinetics in Dendron and Polymer Diads with Dendron−Rod−Coils

species	k_Q(dendron−rod) (ns^{-1})	k_Q(rod−coil) (ns^{-1})	contribution (%) dendron	polymer
G1 dendron−rod−coil **1**	0.23	0.29	44	56
G2 dendron−rod−coil **2**	0.36	0.29	55	45
G3 dendron−rod−coil **3**	0.42	0.29	59	41

steady-state emission of the benzthiadiazole chromophore **17** is measured in the presence of the quencher [(diaryamino)pyrene or naphthalenediimide] at various concentrations. With increasing concentration of the quencher, the emission intensity of the chromophore decreases as one would expect. The fluorescence intensity in the absence (I_0) and presence (I) of either of the quenchers can be related to its concentration ([Q]) using the Stern−Volmer equation $I_0/I = 1 + K_{SV}[Q]$. A plot of I/I_0 vs [Q] affords the Stern−Volmer quenching constant (K_{SV}), which is a measure of the ability of the (diarylamino)pyrene or the naphthalenediimide to quench the excited state of the benzthiadiazole chromophore. K_{SV} is also related to the bimolecular quenching rate constant k_q through $K_{SV} = k_q\tau_0$, where τ_0 is the fluorescence lifetime of the dendrimer in the absence of quenchers. The Stern−Volmer plots for the (diarylamino)pyrene and naphthalenediimide are shown in Figure 10. The plots are linear, and there are no changes in the absorption and emission spectral shapes of the molecules in the mixture. These observations suggest that the observed fluorescence quenching is dynamic, i.e., based on bimolecular collisions. It is clear from the slopes of these lines that the naphthalenediimide **9** is far more effective than the (diarylamino)pyrene **16** at quenching the excited state of the chromophore **17**. It is to be noted that the differences between the photoinduced charge transfer abilities in the dendron−rod vs the rod−coil are relatively minor. Combination of these two observations clearly suggests that the dendritic architecture indeed provides a distinct advantage in the photoinduced electron transfer compared to the polymer coil.

What could be the reason for dendrimers providing this architectural advantage in photoinduced charge transfer over linear polymer coils? We have previously suggested that the high density of functionalities and back-folding in higher generations of dendrimers help boost the efficiency of the electron transfer in these branched molecules.[13] It is interesting to ask whether all charge transfer functionalities in different architectures, such as linear polymers, could participate in the electron transfer process just as in dendrimers. In our polymer backbone, the average number of repeat units is about 15. Thus,

Scheme 4. Synthesis of Model Compounds

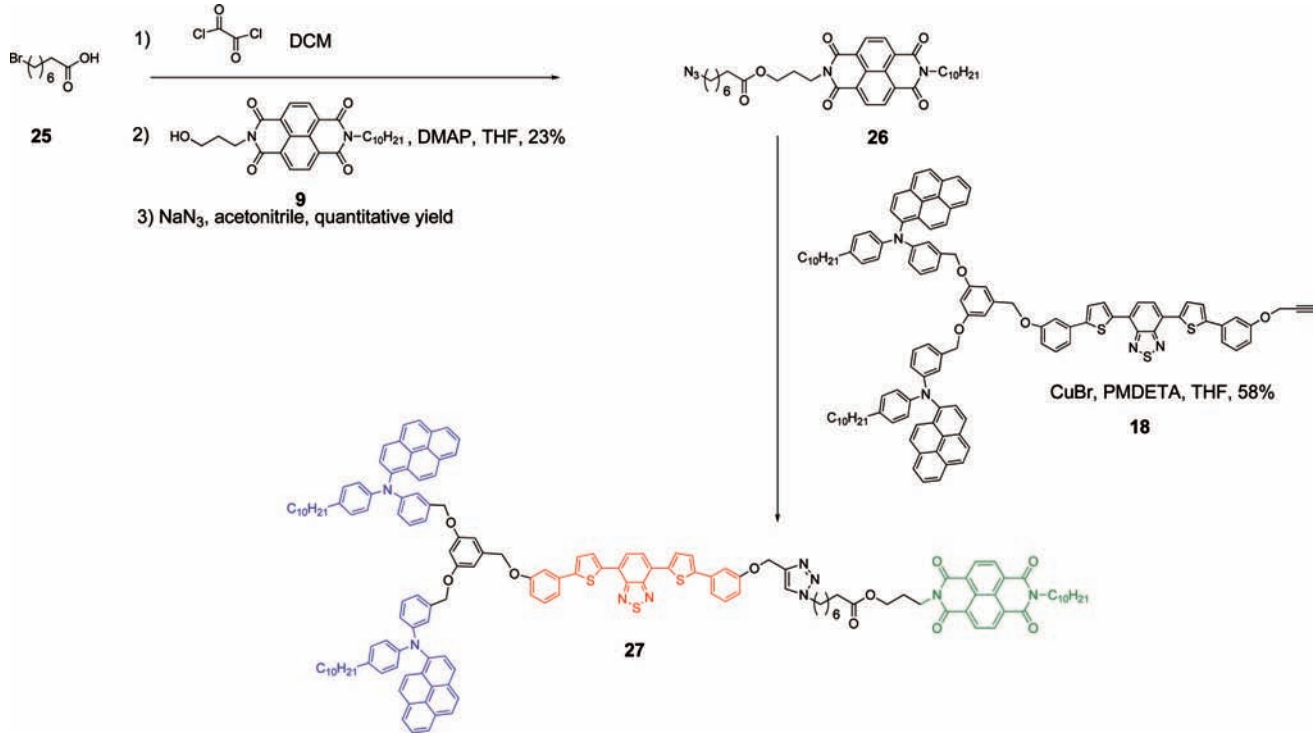

Table 5. Rod Fluorescence Decay (λ_{ex} = 500 nm) and CT Efficiency of Model Compound **27** and G1 Dendron−Rod−Coil **1**

species	A	τ_A (ns)	B	τ_B (ns)	k_Q (ns^{-1})	η_{CT}
model compound **27**	0.21	0.51	0.79	1.95	0.48	0.79
G1 dendron−rod−coil **1**	0.56	0.74	0.44	2.90	0.47	0.79

the number of naphthalenediimide functionalities in the polymer coil is about twice as high as the number of (diarylamino)pyrene units in the G3 dendron. Despite this, combined with the fact that the naphthalenediimide is more capable of photoinduced charge transfer, the efficiency from the polymer coil is only comparable with that of the dendron. It is possible that this is because only the naphthalenediimide functionality closest to the benzthiadiazole chromophore participates in the initial photoinduced charge transfer step, unlike the dendrons. To test this hypothesis, we synthesized a dendron−rod−coil analogue where there is a single naphthalenediimide functionality. The distance between the benzthiadiazole chromophore and the naphthalenediimide functionality in this analogue **27** was kept the same as that with the dendron−rod−coil molecule **1**.

To synthesize **27**, 8-bromooctanoic acid was reacted with oxalyl chloride to convert the acid functionality into acid chloride, which was then treated with hydroxyl-functionalized naphthalenediimide **9** in the presence of DMAP as a catalyst to obtain the bromo-terminated naphthalenediimide derivative. Treatment of this compound with sodium azide afforded naphthalenediimide derivative **26** containing azide functionality. This molecule was then clicked with the acetylenic functionality of the dendron−rod molecule to obtain the single naphthalenediimide molecule analogue for the G1 dendron−rod−coil **1**, as shown in Scheme 4.

The fluorescence decay of the rod in this model compound is shown in Table 5. The η_{CT} and k_Q values for the G1 dendron−rod−coil **1** and its analogue **27** are identical. This indicates that the naphthalenediimide that is closest to the chromophore is the primary participant in the photoinduced charge transfer process in the polymer coil. On the other hand, the population density of functionalities in the dendritic periphery has a positive effect on the charge transfer.[13] Thus, it is reasonable to conclude that the high-density packing and the number of peripheral charge transfer functionalities equidistant from the chromophore are indeed the reasons for the dendritic architectural advantage. Note however that the polymer coil also could play a crucial role in our long-term goals of obtaining microphase-separated structures with a long-lived charge-separated state for photovoltaics.

Conclusions

Considering the advantages of dendritic architectures in photoinduced electron transfer, but issues in moving the charge away from the core due to encapsulation, we have designed and synthesized dendron−rod−coil-based donor−chromophore−acceptor triads for photoinduced charge transfer. We have shown that (i) the combination of the dendron and the polymer coil with a chromophore rod connecting the two is indeed advantageous for photoinduced charge transfer, (ii) dendron−rod−coil-based triads exhibit better efficiencies compared to either the dendron−rod or the rod−coil diad, (iii) on the basis of the efficiencies of the diads, the dendrons and the polymer coil make similar contributions to the overall charge transfer based quenching process, (iv) the polymer coil functionality, naphthalenediimide, is a much better excited-state quencher for the benzthiadiazole chromophore than the (diarylamino)pyrene on the basis of Stern−Volmer quenching studies (this suggests that the dendrons have an architectural advantage over polymer coils for photoinduced charge transfer), (v) although dendrons provide clear advantages in charge transfer quenching, the dendron−rod−dendron triads do not perform better than the donor−chromophore−acceptor triads based on the dendron−rod−coil architecture, and (vi) while all electron donor functionalities in the dendritic periphery can equally participate in the excited-

state quenching of the chromophore rod, the naphthalenediimide electron acceptor unit that is closest to the chromophore is the primary participant in the quenching that arises from the polymer coil. The realistic possibility that dendron−rod−coil structures are capable of providing microphase-separated architectures on the basis of prior literature,[14] combined with our findings here, suggests that these molecules hold great promise in organic photovoltaics. Polymer processing to achieve morphological control, device fabrication, and charge transfer dynamics in the solid state are part of the current focus in our laboratories.

Acknowledgment. We thank the NSF for partial support through the Center for Fueling the Future (Grant CHE-0739227 to S.T.) and Grant CHE-0719039 to C.J.B. and the Army Research Office for support through the Massachusetts Center for Renewable Energy Science and Technology (Grant 54635-CH to S.T.).

Supporting Information Available: Synthetic and other experimental details. This material is available free of charge via the Internet at http://pubs.acs.org.

JA809194U